International Journal of Innovative Research in Engineering and Management (IJIREM)
ISSN (Online): 2350-0557, Volume 13, Issue 1, February 2026
DOI: https://doi.org/10.55524/ijirem.2026.13.1.11
Article ID IJIRE-1441, Pages 87-100
www.ijirem.org

Spatial Econometric Analysis of Biomass Carbon Density Across CD Blocks of North Bengal, India

Asad Ali Sarkar[1], and Sebak Kumar Jana[2]

[1]Research Scholar, Centre for Adivasi Studies and Museum, Vidyasagar University, West Bengal, India
[2]Professor, Department of Economics, Vidyasagar University, West Bengal, India, West Bengal, India

Correspondence should be addressed to Asad Ali Sarkar; hiasadsarkar@gmail.com

Received: 29 January 2026; Revised: 16 February 2026; Accepted: 28 February 2026

Copyright © 2026 Made Asad Ali Sarkar et al. This is an open-access article distributed under the Creative Commons Attribution License, which permits unrestricted use, distribution, and reproduction in any medium, provided the original work is properly cited.

ABSTRACT- Precise quantification of biomass carbon density (BCD) is imperative for localized climate mitigation and sustainable forest governance; however, spatial dependencies at micro-administrative granularities remain critically under-researched. This investigation examines the spatial distribution and multivariable determinants of BCD across 72 administrative CD blocks in North Bengal, West Bengal India—a physiographically diverse region spanning a sharp altitudinal gradient from the Himalayan highlands to the Gangetic plains. The methodological framework used Global Moran's I and Getis-Ord G_i^* statistics to detect spatial autocorrelation, subsequently employing a comparative performance assessment between Ordinary Least Squares regression and the Spatial Lag Model. Empirical results demonstrate substantial positive spatial clustering, with BCD concentrations ranging from 10.75 Mg C/ha, in peri-urban sectors to 627.45 Mg C/ha within montane forest ecosystems. Lagrange Multiplier diagnostics corroborated the statistical superiority of the SLM, which yielded a significant spatial lag coefficient. This indicates that approximately 28% of a block's carbon density is endogenously mediated by the ecological attributes of contiguous administrative units through spatial spillover mechanisms. While forest canopy cover and elevation were identified as the primary positive determinants of carbon sequestration, anthropogenic expansion of impervious surfaces constituted the principal driver of biomass degradation. The study recommends policy frameworks transition toward integrated, landscape-scale management paradigms that prioritize the preservation of high-altitude "carbon cores" and mitigate habitat fragmentation through trans-boundary ecological corridors and green buffers in urbanizing zones.

KEYWORDS: Biomass Carbon Density, Spatial Lag Model, Moran's I, North Bengal, Spatial Spillover, Climate Mitigation, Sustainable Forest Management.

I. INTRODUCTION

Biomass carbon density refers to the quantity of carbon sequestered within the living biomass of an ecosystem per unit land area, conventionally quantified in megagrams of carbon per hectare[19]. BCD is a key indicator in the global carbon cycle. It provides baseline data for assessing sequestration potential and monitoring terrestrial carbon pools. Woody terrestrial biomass accounts for ~83% of Earth's living carbon, with forests storing 70–90% of global aboveground organic carbon[10]. In India, forest biomass comprises nearly 74% of national carbon reserves, thereby underpinning key climate mitigation imperatives, including those embedded in the Paris Agreement[23]. Rigorous BCD appraisal is indispensable for illuminating ecosystem functionalities, tracing temporal shifts in carbon inventories, and crafting land stewardship paradigms to amplify sequestration efficacy[20]. Granular carbon estimations at the administrative block scale are progressively essential for devolving national climate imperatives into bespoke local safeguards[13]. While global and regional biomass mappings provide broad overviews, they typically lack the resolution essential for subnational spatial planning and decentralized forestry management. Fine-scale block- or micro-area-level analyses detect specific anthropogenic pressures—such as urban expansion—and biophysical variables with strong cross-boundary variations [3]. This refined methodology affords sharper diagnoses of woodland attrition, ontogenetic trajectories, and conservation yields, fortifying carbon ledgers and sustainable asset husbandry[11]. Traditional methods like ordinary least squares regression assume that observations are independent and identically distributed. However, this assumption is frequently violated in spatially autocorrelated ecological data, where proximity induces similar attributes and biases statistical inferences[17].

Thus, erudite spatial econometric or geostatistical apparatuses are mandated to delineate these covariances and engender veracious BCD extrapolations across mosaic terrains[8]. In geospatial arrays, this phenomenon—spatial autocorrelation—entails one block's BCD being markedly sculpted by vicinal polities' attributes(D. et al., 1974). Spatial econometric stratagems proffer stalwart countermeasures: spatial autoregressive or spatial lag models embed spatial weighting matrices to operationalize these linkages, facilitating appraisal of spillover phenomena, whereby sylvan vigor or dilapidation in one polity reverberates upon contiguous carbon aptitudes[26].

Despite numerous studies on forest biomass, a significant gap remains in the literature. Most Indian research emphasizes macro-regional surveys or limited plot sampling in the Terai and Himalayan regions [4]. Few

studies apply advanced spatial econometrics to analysed carbon variations at the micro-administrative block level, particularly within North Bengal's diverse socio-ecological landscape [2]. Existing frameworks often overlook cross-boundary spillovers linking montane forests to rapidly urbanizing lowlands.

This study addresses this research gap by examining biomass carbon density across 72 administrative blocks in North Bengal, West Bengal. The region spans a unique physiographic gradient—from the Himalayan highlands of Darjeeling and Kalimpong to the alluvial plains of Jalpaiguri and Malda—integrating remote sensing data, primarily the Normalized Difference Vegetation Index, with spatial econometric models. Thus, it provides a spatially explicit analysis of biophysical and anthropogenic drivers influencing carbon distribution in one of India's key ecological corridors. The research objectives of this study are as follows:

- To estimate the spatial distribution of biomass carbon density across the 72 administrative Blocks of North Bengal.
- To assess the global and local spatial autocorrelation of biomass carbon density.
- To identify the physical, biophysical and anthropogenic drivers of carbon variation by comparing the performance of Ordinary Least Squares Regression—a global model—with the Spatial Autoregressive Model.
- To quantify the direct and indirect impacts of environmental and anthropogenic factors on regional biomass stocks, thereby elucidating the influence of carbon dynamics in one administrative CD block on the ecological health of neighbouring units.

II. STUDY AREA

The study area encompasses a physiographic transect ranging from the northern high-altitude Himalayan ranges to the low-lying alluvial Gangetic plains in the south[1] [14]. Community development blocks across this region are situated within the districts of Darjeeling, Kalimpong, Jalpaiguri, Alipurduar, Cooch Behar, North Dinajpur, South Dinajpur, and Malda [5] [25]

A. Geographical and Topographical Profile of the Study Area

The region exhibits a strong altitudinal gradient [Figure 1], with elevations ranging from about 3,660 m in the northern Himalayan front across the Darjeeling and Kalimpong hills to nearly 30–50 m above sea level in the southern plains. Physiographically, the region may be categorized into three primary zones: the Himalayan Highlands, encompassing the northernmost blocks of Darjeeling and Kalimpong districts and defined by steep slopes and deep valleys[25] the Terai and Dooars, manifesting as a piedmont belt along the Himalayan foothills that includes tectonic blocks and broad alluvial fans formed by major rivers such as the Teesta, Jaldhaka, and Torsa [1] [5][9] and the North Bengal Plains, consisting of a low-lying flat alluvial expanse extending southward across Malda and Dinajpur districts, wherein intensive agricultural practices prevail[18] [24].

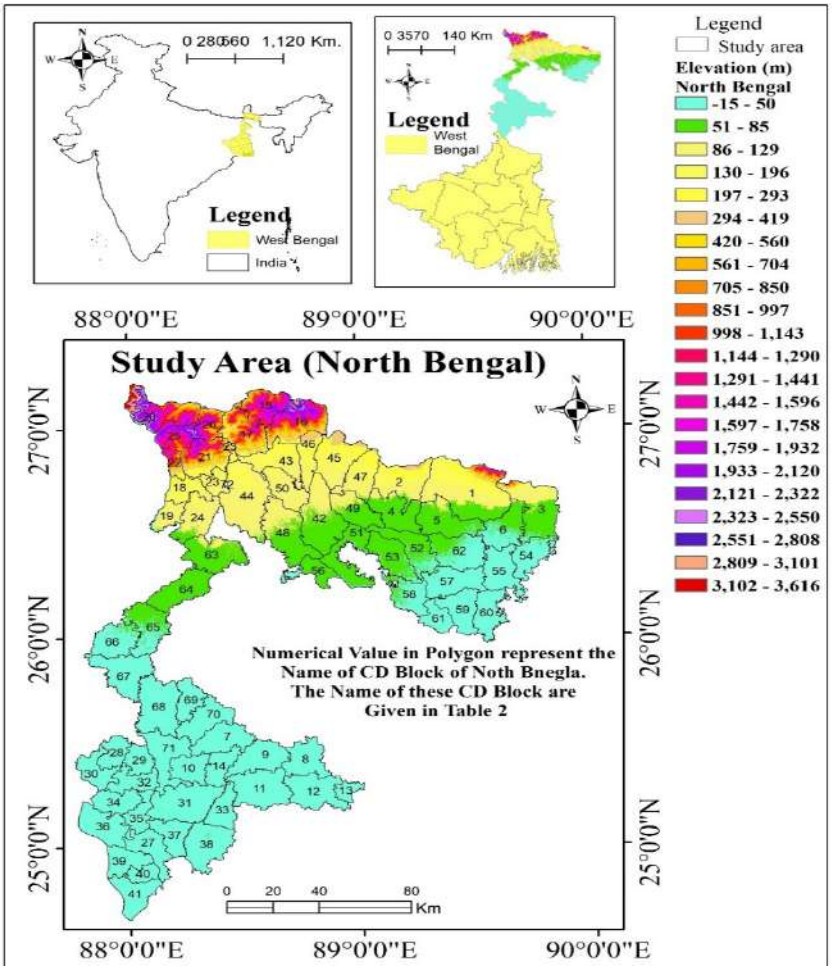

Figure 1: Study Area: North Bengal, West Bengal, India

B. Climatic Conditions

The study area exhibits a subtropical monsoonal climate and ranks among India's highest-precipitation regions, with annual rainfall ranging from 2,500 to 3,900 mm[18]. Approximately 78% of this precipitation occurs during the Southwest Monsoon[21]. Temperature profiles vary markedly with elevation: the southern plains register summer maxima of 38°C, while the northern highlands record winter minima of 3°C or below [18].

C. Natural Vegetation and Land Use/Land Cover

The topographic and climatic heterogeneity prevalent in the region fosters a diverse spectrum of vegetation assemblages, profoundly shaping biomass carbon density profiles. Forest canopies transition from multi-stratified tropical evergreen complexes to moist deciduous formations, wherein Shorea robusta predominates the latter [16][18]. Within the Terai and Dooars belts, expansive tea plantations constitute pivotal agro-ecosystems, materially augmenting the aggregate regional carbon reservoir [1] [5]. In contrast, southern community development blocks are defined by rigorous agrarian pursuits across the Indo-Gangetic alluvial lowlands, concomitant with expeditious urbanisation converting verdant expanses to impervious built environments, particularly in Matigara and Rajganj [7]. Scrutiny of the 72 administrative blocks elucidates the confluence of biophysical and anthropogenic determinants modulating biomass carbon density spatiality, while precipitating cross-jurisdictional spillover dynamics throughout North Bengal.

III. DATABASE AND VARIABLES

The paper adopts robust Spatial Autoregressive model in place of traditional regression techniques, thereby effectively accounting for pronounced spatial dependencies and quantifying the 28% spillover effect across administrative boundaries. By employing high-resolution geospatial datasets and the Spawn and Gibbs biomass map, the study delivers a detailed block-level analysis that delineates critical carbon hotspots and coldspots with robust statistical validity. A primary methodological limitation concerns the temporal misalignment between the dependent variable and the independent variables. The analysis employs the 2010 Spawn and Gibbs dataset for biomass carbon density [27], whereas the biophysical and anthropogenic drivers pertain to the more recent 2021–2024 period. Although the 2010 dataset constitutes the globally harmonized reference standard for integrated above- and below-ground biomass [27], this 11- to 14-year discrepancy may not fully account for recent forest degradation or the accelerated urban expansion observed in the Siliguri corridor over the past decade. Nevertheless, given that mature Himalayan forest structures exhibit gradual change at decadal timescales, the 2010 data remain a reliable structural baseline for examining the region's spatial clustering patterns[14][23].

A. Dependent Variable:

The dependent variable in this study is Biomass Carbon Density (BCD), quantified in megagrams of carbon per hectare (Mg\/C ha^(-1)) [10] [27]. This unit denotes the mass of carbon stored in both aboveground and belowground living organic matter [10], where one megagram is equivalent to one metric tonne[27].

BCD data were obtained from the India Biodiversity Portal, an integrated platform for geospatial biodiversity informatics in India. The specific raster dataset, originally developed by Spawn and Gibbs, provides global high-resolution maps of BCD for the year 2010 (Spawn et al., 2020). Researchers, including Arjun Srivathsa, Thomas Vattakaven, and R. Prabhakar, employed this dataset to prioritize Indian landscapes based on ecosystem services. This study extracted the raster values to calculate the mean value of BCD at the administrative block level across the 72 blocks of North Bengal; this mean value served as the primary dependent variable.

B. Independent Variables

The selection of these variables follows established research showing that tree cover and NDVI are primary positive predictors of biomass, while built-up area expansion is a leading driver of carbon loss [28].

Table 1: Specification of Geospatial and Anthropogenic Drivers of Biomass Carbon Density

	Variable	Data Source / Processing	Description / Rationale
Biophysical	NDVI	Landsat 8 OLI imagery	Proxy for vegetation Vigor and photosynthetic activity; positively correlated with biomass accumulation
	% Tree-covered area (TREE)	LULC map (2017–2024) from Living Atlas; zonal statistics in ArcGIS 10.8	Enhances biomass carbon density via increased vegetation cover
Anthropogenic	% Built-up area (BUTC)	LULC map (2017–2024) from Living Atlas; zonal statistics in ArcGIS 10.8	Anthropogenic pressure reduces biomass carbon density through land conversion[28]
Climatic	Average maximum temperature (TEMP)	CRU TS 4.09 gridded data (2021–2024)	Optimal temperature regimes promote photosynthesis and biomass growth
	Annual rainfall (RAIN)	CRU TS gridded data (aligned with temperature period)	Controls ecological limits for forest growth and carbon accumulation
Physical	Elevation (ELVN)	Digital elevation model	Elevation is a key abiotic factor influencing canopy structure and biomass distribution.

Land use/Land Cover (LULC) raster data for the study area were processed to compute CD Block-level areas for each category, which were tabulated in Excel. Mean CD Block-level elevation was derived from a digital elevation raster map using the Zonal Statistics as Table tool in ArcGIS 10.8. CD Block-level temperature and rainfall were extracted similarly; the six variables were then joined to the shapefile of the North Bengal CD Block map [Figure 1] in ArcGIS 10.8.

IV. METHODOLOGY

A. Spatial Autocorrelation Analysis

Spatial dependence in the BCD distribution was assessed using Global Moran's I to quantify the overall degree of clustering across the administrative CD blocks(Salinas-Pérez et al., 2024; Tsui et al., 2022). Subsequently, Anselin's Local Moran's I was applied to detect local spatial associations, particularly "High-High" and "Low-Low" clusters; A high positive Local Moran's I value signifies that an administrative block is surrounded by neighbours exhibiting similar carbon density levels; whereas negative values denote spatial outliers.

Global Moran's I- Global Moran's I measure [Eq. 1] the overall spatial dependence and degree of clustering of BCD across the study area

$$GMI = \frac{n\sum_{i=1}^{n}\sum_{j=1}^{n} w_{ij}(x_i-\bar{X})(x_j-\bar{X})}{(\sum_{i=1}^{n}(x_i-\bar{X})^2)(\sum_{i=1}^{n}\sum_{j=1}^{n} w_{ij})} \quad \text{(Eq. 1)}$$

Anselin Local Moran's I- The Local Moran's I identifies[Eq. 2- Eq. 4] specific local spatial associations, classified as "High-High," "Low-Low" clusters, or spatial outliers.

$$I_i = \frac{x_i-\bar{X}}{S_i^2}\sum_{j=1,j\neq i}^{n} w_{ij}\left(x_j-\bar{X}\right) \quad \text{(Eq. 2)}$$

where the variance S_i^2 is defined as:

$$S_i^2 = \frac{\sum_{j=1,j\neq i}^{n}(x_j-\bar{X})^2}{n-1} \quad \text{(Eq. 3)}$$

$$S^2 = \frac{\sum_i (x_i-\bar{x})^2}{n-1} \quad \text{(Eq. 4)}$$

Here, x_i expressed the BCD for block , x_j for neighbouring block j, Xˆis the mean BCD, and w_ij is the spatial weight between them. A positive I_i indicates a CD block surrounded by similar BCD values (clusters), while a negative value indicates an outlier surrounded by dissimilar values. Statistical significance is assessed via Z-score, enabling classification into High-High, Low-Low, High-Low, and Low-High categories. I_i : Local Moran's I value for block i. x_i: Attribute value for target CD block i; x_j : value for neighbouring block j . w_ij: Spatial weight signifying relationship intensity between i and j (Lian et al., 2012).

Getis-Ord Gi* Spatial Hotspot Analysis- To complement the Local Moran's I and provide a more granular assessment of carbon clustering, the Getis-Ord G_i^* statistic was used. This method identifies statistically significant "hot spots" and "cold spots" by evaluating each administrative block within the context of its neighbours. While Moran's I method identifies general spatial associations, the G_i^*statistic specifically measures the intensity of clustering for high and low values. The G_i^* statistic is indicated as a Z-score, calculated using the following formula[Eq. 5]

$$G_i^*(d) = \frac{\sum_{j=1}^{n} w_{ij}(d)x_j - \bar{x}\sum_{j=1}^{n} w_{ij}(d)}{S\sqrt{\frac{\left[n\sum_{j=1}^{n} w_{ij}^2(d) - \left(\sum_{j=1}^{n} w_{ij}(d)\right)^2\right]}{n-1}}} \quad \text{(Eq. 5)}$$

where, x_j is the BCD value for block j, w_ij is the spatial weight, n is the number of CD blocks, and xˆ and S expressed the mean and standard deviation of BCD across the study area (Chang et al., 2015; Lang et al., 2023). Hot Spots: A statistically significant positive Z-score indicates that a block with high carbon density is surrounded by other high-value blocks, forming a "Hot Spot" (e.g., the northern Himalayan belt in the map at < 0.01). Cold Spots: A st atistically significant negative Z-score represent a "Cold Spot," where low BCD values are spatially clustered, indicating regions of severe biomass depletion (e.g., the southern plains at p 0.10).

B. Ordinary Least Squares Regression

Ordinary Least Squares Regression (OLS) regression serves as the baseline global model for this study. However, its validity depends on the assumption that observations are independent and identically distributed (Gorrell et al., 2023). As noted in the methodology for spatial autocorrelation, ecological data often violate this assumption through spatial dependence. In such cases, OLS yields biased and inefficient estimates, failing to account for how its neighbours influence the carbon density of one CD block[22] Taylor et al., 2015). The formula for multiple linear regression is[Eq. 6]:

$$y_i = \sum_{q=1}^{Q} X_{iq}\,\beta_q + \epsilon_i \quad \text{[Eq. 6]}$$

Where: y_i represent the dependent variable (Biomass Carbon Density) for observation i. X_iq express the q-th independent explanatory variable (such as tree cover, elevation, or vegetation indices) for observation i. β_q is the regression coefficient that quantifies the impact of the q-th explanatory variable on the dependent variable. ϵ_i express the error term or residual for observation i, representing the portion of y_iunexplained by the model. Q: The total number of explanatory variables (including the intercept). In matrix notation, the OLS model is represented as:

$$y = X\beta + \epsilon \quad \text{[Eq. 7]}$$

where: y is an n ×1 vector of observations on the dependent variable, X is an n ×Q matrix of observations on the explanatory variables (including a column of ones for the intercept), β is a Q ×1 vector of parameters to be estimated, ϵ is an n ×1 vector of error terms. The error term (residual) for each observation can also be expressed as[Eq. 8]:

$$\epsilon_i = y_i - \sum_{q=1}^{Q} X_{iq}\,\beta_q \quad \text{[Eq. 8]}$$

While OLS provides a global overview of environmental effects, research indicates it is often not appropriate for regional biomass modelling if the data exhibit significant spatial autocorrelation, as the model cannot account for spatial variations and dependencies within the residuals[22] [28].

C. Spatial Econometric Modelling: Spatial Lag Model

To address the limitations of the ordinary least squares model and capture spatial spillover effects, a spatial lag

model (SLM), also known as the spatial autoregressive (SAR) model, was employed [12][15].

The SAR incorporates a spatial weight matrix (W) to account for the influence of neighbouring administrative CD blocks on local biomass carbon density. The model is specified as[27]:

$$y = \rho Wy + X\beta + \epsilon \quad \text{[Eq. 9]}$$

or, in expanded form with intercept:

$$y = \alpha \iota_n + \rho Wy + X\beta + \varepsilon \quad \text{[Eq. 10]}$$

where: y: (n×1) vector of biomass carbon density (BCD) for each CD Block; W:(n×n) spatial weights matrix; ρ: spatial autoregressive coefficient reflecting the intensity of spatial dependence (spatial spillover); Wy: spatial lag term representing the weighted average BCD of neighbouring blocks; X: (n×K) matrix of independent explanatory variables; β: (K×1): vector of coefficients associated with the explanatory variables; α: intercept (constant term); ι_n:(n×1) vector of ones; ϵ: (n×1) vector of error terms. A positive and statistically significant (ρ) indicates the presence of positive spatial dependence - i.e., the BCD in one block is positively influenced by the BCD in neighbouring blocks.

V. RESULTS

A. Analysis of Block-wise BCD Distribution

The block-wise distribution of BCD across North Bengal (Table 2) varied widely, ranging from a low of 10.750 Mg\/C ha^(-1) in Matigara Rajganj to a high of 627.454 Mg\/C ha^(-1) in Gorubathan Table 2. This variation indicates substantial spatial heterogeneity ascribable to the region's diverse ecological and physiographical features.

5.1.1 High-Density Carbon Reservoirs

Analysis divulges a pronounced concentration of high BCD values in the northernmost CD Blocks of West Bengal. This "High-Density Zone," depicted by dark green shades in Figure 2, encompasses the CD blocks with the highest BCD values: Gorubathan (627.454 Mg\/C ha^(-1); the maximum in the study area), Rangli-Rangliot (541.604 Mg\/C ha^(-1)), Kalimpong II (534.045 Mg\/C ha^(-1)), Darjeeling Pulbazar (520.037 Mg\/C ha^(-1)), and Kurseong (480.521 Mg\/C ha^(-1)). Located in the high-altitude Himalayan region, these CD blocks display elevated BCD owing to dense, mature forest cover and relatively lower anthropogenic disruption than in the plains.

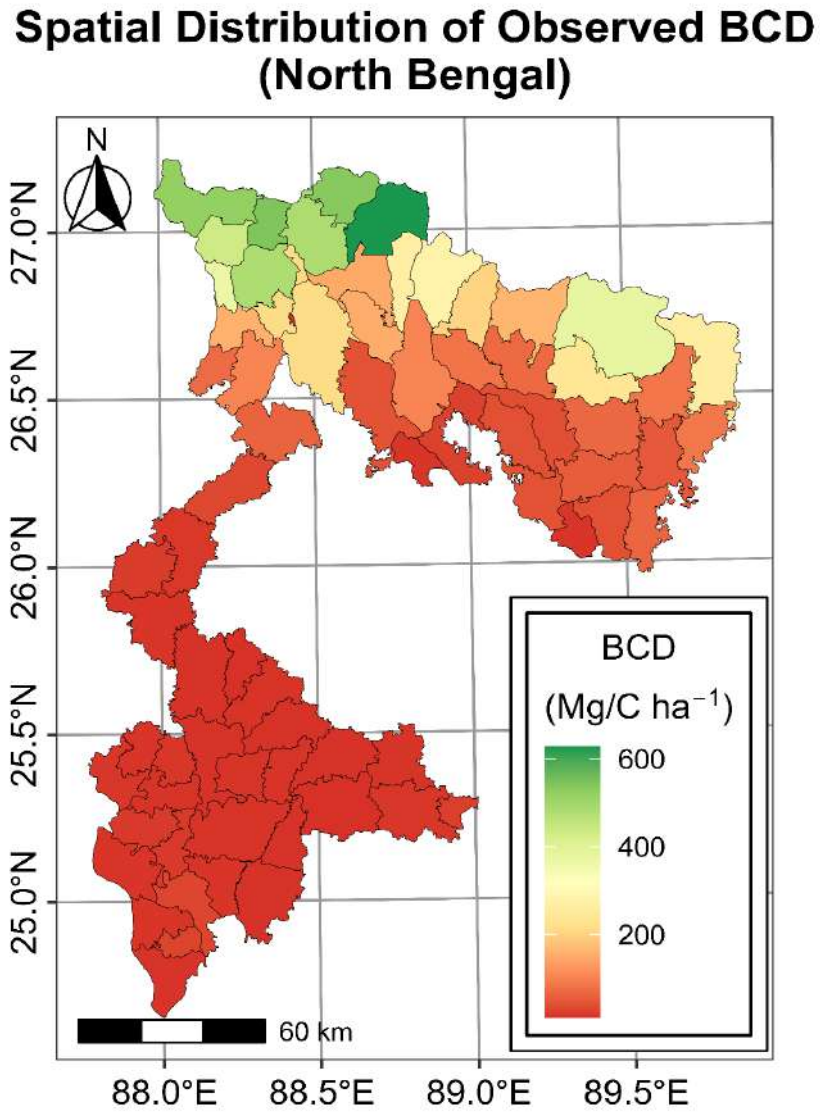

Figure 2: Spatial Distribution of Observed Biomass Carbon Density across 72 CD Blocks of North Bengal.

Table 2: Estimated Biomass Carbon Density (Mg\/C ha^(-1)) for the 72 Administrative Blocks of North Bengal

SL. No	Name of CD Block	Mean BCD	SL. No	Name of CD Block	Mean BCD	SL. No	Name of CD Block	Mean BCD
1	Kalchini	377.779	25	Jorebunglow-Sukhiapokhri	436.191	49	Dhupguri	84.065
2	Madarihat	163.142	26	Rangli-Rangliot	541.604	50	Kranti	151.762
3	Kumargram	260.896	27	English Bazar	30.409	51	Mekhliganj	26.562
4	Falakata	70.352	28	Harishchandrapur I	15.282	52	Mathabhanga II	39.336
5	Alipurduar I	238.729	29	Chanchal I	16.191	53	Mathabhanga I	41.562
6	Alipurduar II	86.574	30	Harishchandrapur II	16.785	54	Tufanganj II	87.185
7	Kushmundi	13.522	31	Gazole	13.879	55	Tufanganj I	50.945
8	Kumarganj	14.450	32	Chachal II	13.582	56	Haldibari	14.829
9	Gangarampur	12.791	33	Bamangola	13.306	57	Cooch Behar I	56.599
10	Harirampur	14.521	34	Ratua I	18.753	58	Sitalkuchi	43.922
11	Tapan	12.457	35	Ratua II	18.747	59	Dinhata I	41.869
12	Balurghat	16.726	36	Manikchak	15.908	60	Dinhata II	66.191
13	Hilli	23.949	37	Old Malda	15.167	61	Sitai	16.021
14	Bansihari	14.000	38	Habibpur	12.986	62	Cooch Behar II	69.278
15	Kalimpong II	534.045	39	Kaliachak II	15.472	63	Chopra	63.236
16	Gorubathan	627.454	40	Kaliachak I	29.138	64	Islampur	33.056
17	Kalimpong I	484.099	41	Kaliachak III	14.174	65	Goalpokhar I	18.159
18	Naxalbari	156.607	42	Maynaguri	103.192	66	Goalpokhar II	21.438
19	Khoribari	72.957	43	Mal	149.025	67	Karandighi	15.116
20	Darjeeling-Pulbazar	520.037	44	Rajganj	212.334	68	Raiganj	12.929
21	Kurseong	480.521	45	Nagrakata	276.784	69	Hemtabad	12.723
22	Mirik	367.505	46	Matiali	268.958	70	Kaliganj	14.000
23	Matigara	212.733	47	Banarhat	202.421	71	Itahar	13.344
24	Phansidewa	104.049	48	Jalpaiguri Sadar	44.043	72	Matigara Rajganj	10.750

Moderate-Density Transition Reservoirs- The central portion of West Bengal, illustrated by light green and yellow shades in Figure 2, constitutes a moderate-density transition zone characterized by substantial BCD values, although lower than those in the mountainous regions. Prominent CD blocks within this zone include Kalchini, Matiali, Kumargram, and Banarhat. These areas, encompassing the Terai and Duars regions, comprise protected forest areas, tea gardens, and plantations. Although they sustain considerable biomass levels, the density remains inherently lower than that observed in the primary montane forests of the northern sector.

5.1.3 Low-Density Carbon Reservoirs

The southern and southwestern Blocks, depicted by red and orange shades in Figure 2, exhibit substantially lower carbon stocks. The Blocks with the lowest BCD values are Matigara Rajganj, Tapan, Hemtabad, Gangarampur, and Habibpur. Situated in the plains, these areas display low BCD values attributable to intensive agricultural land use, high population density, and extensive urbanization, all of which have replaced natural biomass with artificial surfaces and croplands.

Evaluating the 72 CD blocks collectively in Figure 2 discloses clear spatial patterns. The most prominent feature is a north-to-south gradient, where carbon density continuously decreases from the northern areas to the southern parts of the landscape. Additionally, the distribution shows strong spatial clustering, with high BCD values forming grouped clusters rather than emerging randomly, while the southern region is dominated by a continuous cluster of low-BCD CD blocks. Certain blocks, such as Jorebunglow-Sukhiapokhri and Mirik, act as important geographical connectors, linking the high carbon density zones of the northern peaks with the gradually declining foothill regions.

Table 3: Results of Global Moran's I Test for Spatial Autocorrelation of BCD

Statistic	Value
Moran's *I*	0.7984
Expectation	-0.0141
Variance	0.0066
Z-value	9.9897
P-value	<2e-16

B. Spatial Autocorrelation Analysis: Global Moran's I

To determine if the geographical distribution of biomass carbon density is statistically clustered, the Global Moran's I was calculated.

To determine if the geographical distribution of biomass carbon density is statistically clustered, the Global Moran's I was calculated, and the results derived from the scatterplot and accompanying Table 3 indicate a Global Moran's I statistic of 0.7984, accompanied by a highly significant z -score of ≈9.99 ($p < 0.001$). The elevated positive value of Moran's I confirms strong positive spatial autocorrelation, demonstrating that BCD is not randomly distributed across North Bengal. Rather, high-BCD Blocks cluster near other high-BCD Blocks, while low-BCD Blocks cluster near other low-BCD Blocks. The z -score of 9.99 indicates that the probability of this clustering occurring by chance is less than 0.1%.

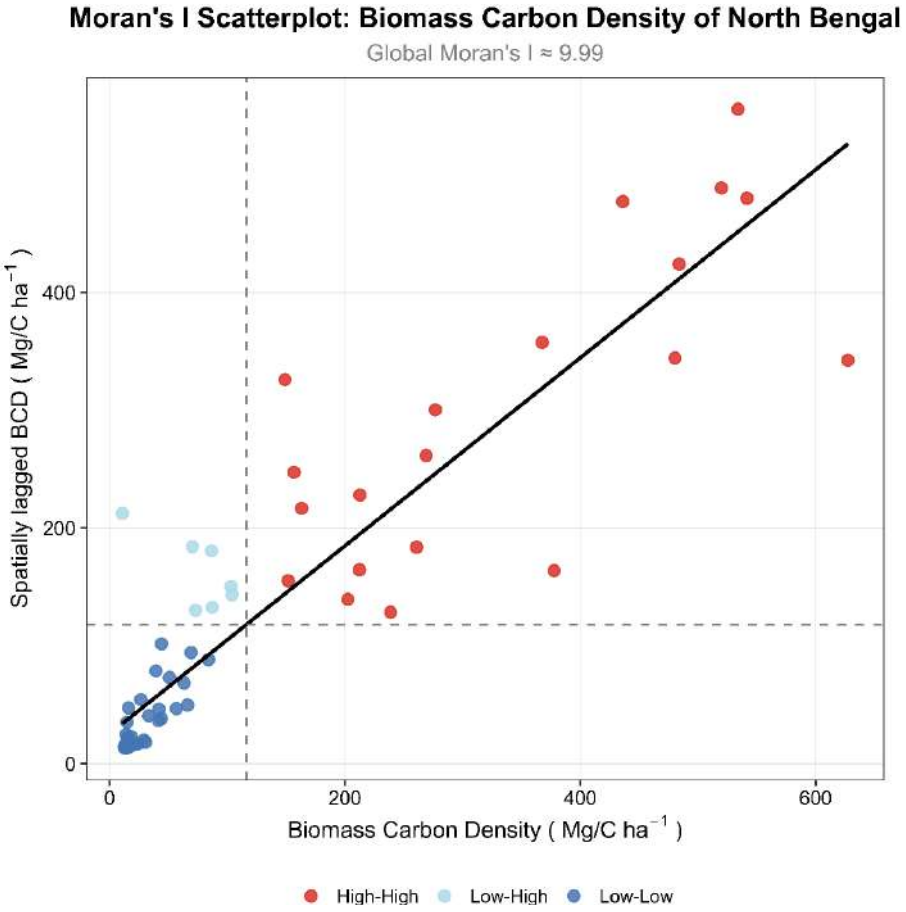

Figure 3: Moran's I Scatterplot for Biomass Carbon Density

The scatterplot Figure 3 expressed the relationship between a CD block's BCD and its spatially lagged BCD, defined as the average BCD of its neighbouring CD blocks. High-High clusters denote hotspots featuring elevated BCD values contiguous with neighbouring Blocks with comparably high BCD levels, and such clusters align with northern hilly regions, encompassing CD blocks such as Gorubathan, Kalimpong I, and Darjeeling-Pulbazar, which collectively form a continuous high-capacity carbon reservoir. Low-Low clusters represent coldspots characterized by low BCD values in CD blocks contiguous with neighbouring Blocks with similarly low BCD values, and such clusters predominate in the southern plains, exemplified by Tapan, Habibpur, and Gangarampur, and where intensive agriculture and urbanization have substantially eroded regional carbon storage capacity. Low-High outliers represent
spatial outliers, characterized by Blocks with low BCD values encircled by neighbours exhibiting high BCD levels, potentially signifying localized deforestation or urban encroachment amid expansive forested landscapes.

C. LISA Cluster Map Analysis

The Local Indicators of Spatial Association cluster map Figure 4 delineates the local spatial autocorrelation of BCD across the 72 CD blocks of North Bengal, providing a spatial disaggregation of the Global Moran's I analysis. Figure 5 illustrates a visual representation of these clusters, identifying statistically significant areas of High-High, Low-Low, High-Low, and Low-High clustering Figure 5.

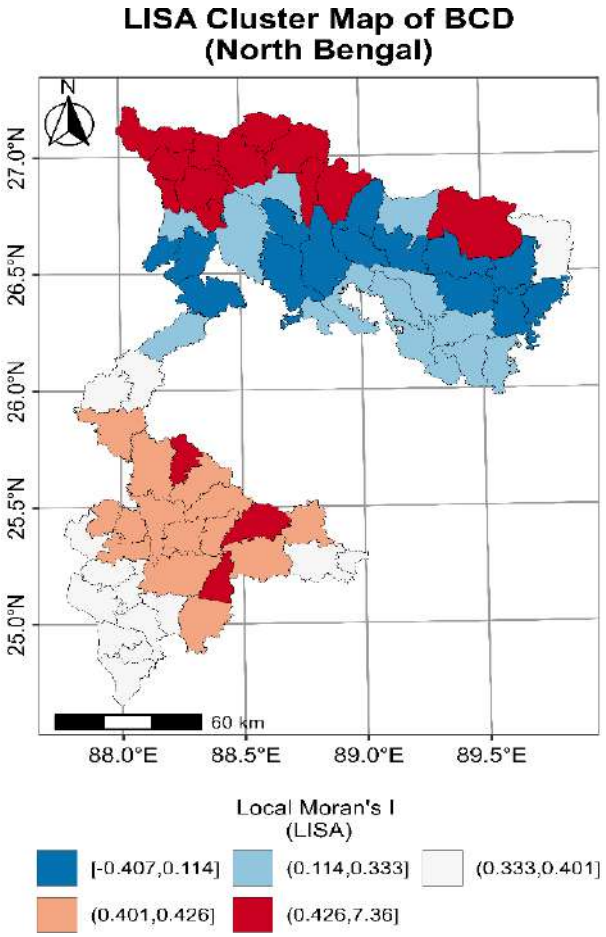

Figure 4: LISA Moran's Map of Biomass Carbon Density

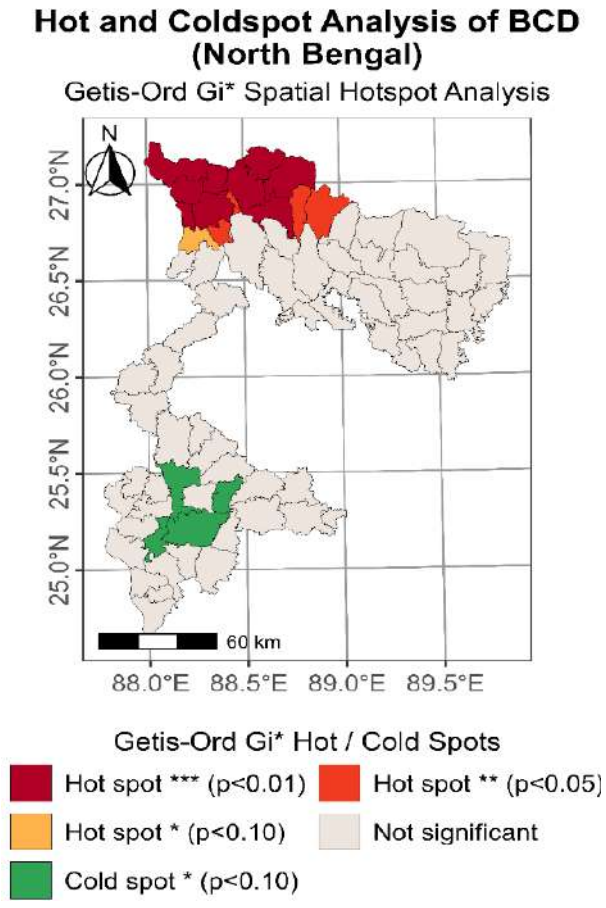

Figure 5: LISA Moran's Map of Biomass Carbon Density

High-High Carbon Hotspots- The northernmost areas, illustrated in dark red on the LISA cluster map [Fig. 4], delineate significant high-high clusters, wherein Blocks exhibit elevated BCD values contiguous with neighbouring Blocks with comparably high BCD values (positive local Moran's I). This pattern substantiates the Himalayan forest belt as a continuous high-capacity carbon reservoir exhibiting substantial spatial spillovers.

Low-Low "Coldspots"- The southernmost areas, illustrated in orange on the LISA cluster map, delineate significant low-low clusters, wherein CD blocks exhibit low BCD values contiguous with neighbouring CD blocks with comparably low BCD values (positive local Moran's I). These clusters correspond to agricultural plains and urbanizing zones characterized by regionally diminished carbon density.

Low-High and High-Low Outliers; Not Significant- Areas shaded in blue indicate low-high and high-low outliers, characterized by negative local Moran's I values—wherein a block's BCD markedly deviates from those of its neighbours—or non-significant clusters exhibiting local Moran's I values near zero. These patterns predominantly emerge at the transitional interfaces between high-elevation forests and low-elevation plains, attributable to localized deforestation, urban expansion, or stochastic variation.

The pronounced high-high and low-low clustering evident in the LISA cluster map—disaggregating the global Moran's of 0.7984 Table 3—constitutes robust empirical evidence for strong positive spatial autocorrelation and dependence in terms of BCD distribution. This pattern is consistent with moving from Ordinary Least Squares to the Spatial Lag Model; Lagrange Multiplier diagnostics indicate both strong lag dependence (LM-Lag: 8.678,; Robust LM-Lag: 4.736,; table not shown) and error dependence as significant (table not shown).

Block conservation policies were also found to be mediocre and biased due to demonstrated interdependence of BCD between neighbouring Blocks - selective protection is a priority for HH hotspots (e.g., Gorubathan, Kalimpong I) to conserve core sinks. In contrast, active restoration is required for LL coldspots (e.g., Tapan, Habibpur) for increasing functional landscape connectivity, reducing fragmentation and enhancing regional carbon sequestration. The analysis reveals a strong latitudinal gradient, with geographic dependence in the northern CD Blocks for high-density carbon reservoirs.

D. Ordinary Least Squares Regression

Given the significant spatial autocorrelation confirmed by the Moran's I analysis and local cluster analysis, traditional OLS regression yields biased and inefficient estimates due to omitted spatial dependence that violates the independence assumption (Gorrell et al., 2023). Therefore, to accurately model the relationships between BCD and its variables, spatial regression techniques accounting for spatial dependencies are warranted.

An Ordinary Least Squares regression was applied to determine the relationships between BCD and its geospatial and anthropogenic variables. This model provides a basis for carbon storage dynamics analysis across North Bengal.

The OLS model exhibits substantial explanatory power, with an adjusted R^2 of 0.924, indicating that

approximately 92.4% of the spatial variation in BCD across the 72 CD blocks the six independent variables account for. The F-statistic of 145.145 ($p < 0.001$) confirms the overall significance of the model, demonstrating that the associations between the dependent and independent variables are not attributable to random variation. The regression coefficients indicate the direction and magnitude of each variable's influence on North Bengal's carbon stocks:

Tree Cover: This is the most potent positive driver. The result means that with every 1% increase in the tree-covered area within a Block, the model suggests an average gain of roughly 4.35 carbon density. This high sensitivity suggests that forest density is a major driver of carbon sequestration capacity in North Bengal.

Table 4: Baseline Ordinary Least Squares Regression Estimates for BCD Drivers

Variable	Estimate	Std. Error	t value	p-value
(Intercept)	857.590***	222.947	3.847	<0.001
NDVI	324.802*	125.754	2.583	0.012
BUTC	-46461.969*	17532.630	-2.650	0.010
TREE	43538.543***	5025.856	8.663	<0.001
RAIN	0.073**	0.027	2.677	0.009
TEMP	-32.519***	6.993	-4.650	<0.001
ELVN	0.177***	0.026	6.755	<0.001
R^2: 0.931 **Adj. R^2:** 0.924 **F-statistic:** 145.145 Significance: *** p < 0.001, ** p < 0.01, * p < 0.05				

Built-up Area: This coefficient reveals a massive trade-off. Every 1% expansion of impervious surfaces (buildings, roads) results in a loss of roughly 4.64 Mg\/C ha^(-1). Critically, the negative impact of urbanization is slightly larger than the positive impact of tree cover, suggesting that urban sprawl destroys carbon faster than typical reforestation can replace it.

Environmental Factors: Elevation (β= 0.177) and Rainfall (β= 0.073): These numbers reflect the "Himalayan advantage." For every 100-meter gain in altitude, a Block naturally gains 1.77 Mg/C ha^(-1) of BCD, while every 100 mm increase in annual rainfall adds 0.73 Mg\/C ha^(-1). These variables define the biophysical ceiling of the northern "carbon core". Temperature (β= -32.519): In the OLS framework, higher temperatures appear detrimental, with every 1^∘ C increase associated with a 3.25 Mg\/C ha^(-1) drop in carbon density. However, as shown in the SAR model, this is a statistical illusion. Vegetation Index NDVI demonstrates a significant positive association (β= 324.802,p = 0.012), validating the satellite-derived vegetation index as a reliable proxy for monitoring carbon density in this landscape.

E. Model Selection: Lagrange Multiplier Diagnostics

While the OLS model shows high explanatory power (Adj. R^2=0.924), the diagnostic tests in Table 5 reveal significant spatial dependence in the residuals. The Lagrange Multiplier tests—specifically the LM-Lag (8.678, p = 0.003)—justify the transition to the Spatial Lag Model. The SAR model addresses the OLS limitations by incorporating a spatial lag coefficient (ρ= 0.295), which formally quantifies the "carbon benefit" shared between adjacent administrative units.

This result serves as the statistical justification for transitioning from the global OLS model to the Spatial Lag Model (SAR), which formally quantifies how much "carbon benefit" is shared between adjacent administrative CD Blocks.

F. Spatial Autoregressive Model

The SAR model was used because it considers the spatial dependency detected by Lagrange Multiplier diagnostics. The SAR model is similar to the OLS model except that this model adopts the Spatial Lag , which represents the weighted sum of neighbouring blocks' biomass carbon density on the local block. The SAR model has an outstanding performance in converting the regional carbon continuity (fitted BCD distribution, as shown in table 5), which implies neighbouring blocks share similar ecological conditions.

Table 5: Spatial Autoregressive Model Estimation Results for Biomass Carbon Density Drivers

Variables	Coefficient	Std. Error	z-value	p-value	
(Intercept)	279.042	264.370	1.055	0.291	ns
NDVI	313.532	112.729	2.781	0.005	***
BUTC	-36,634.579	16,109.630	-2.274	0.023	**
TREE	41,357.958	4,546.887	9.096	<0.001	***
RAIN	0.057	0.026	2.251	0.024	**
TEMP	-13.414	8.635	-1.553	0.120	ns
ELVN	0.118	0.027	4.344	<0.001	***
Spatial Lag (Rho)	0.295	0.095	3.097	0.002	***
Log Likelihood: -366.268 | AIC: 750.536 | Observations: 72 | Sigma²: 1500.429 | LM residual p-value: 0.354					

The Spatial Lag (ρ= 0.295)

The spatial lag coefficient (ρ) provides the most significant implication for policy. It demonstrates a 29.5% neighbourhood effect: if a block's neighbours increase their average carbon density by Mg\/C ha^(-1), that CD block will "automatically" see a gain of nearly 3 Mg\/C ha^(-1) through ecological spillovers, such as improved microclimatic stability and seed dispersal. After controlling for spatial spillovers, the following variables remain significant drivers of BCD:

Tree Cover- The tree covered area remains the strongest positive predictor (β= 41,357.958,p < 0.001). This high coefficient underscores that forest density is the primary driver of carbon storage in the northern highlands.

Built-up Area- Built-up has significant negative impact on carbon stocks (β= -36,634.579,p = 0.023). This indicates that urban expansion and infrastructure development are the leading causes of biomass degradation in the region.

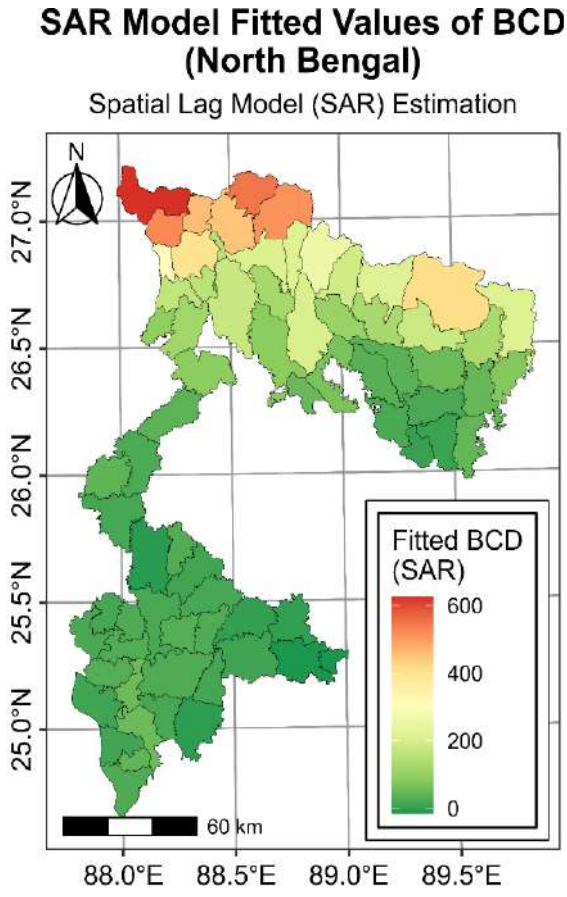

Figure 6: Spatial Autoregressive Model Predicted Carbon Density

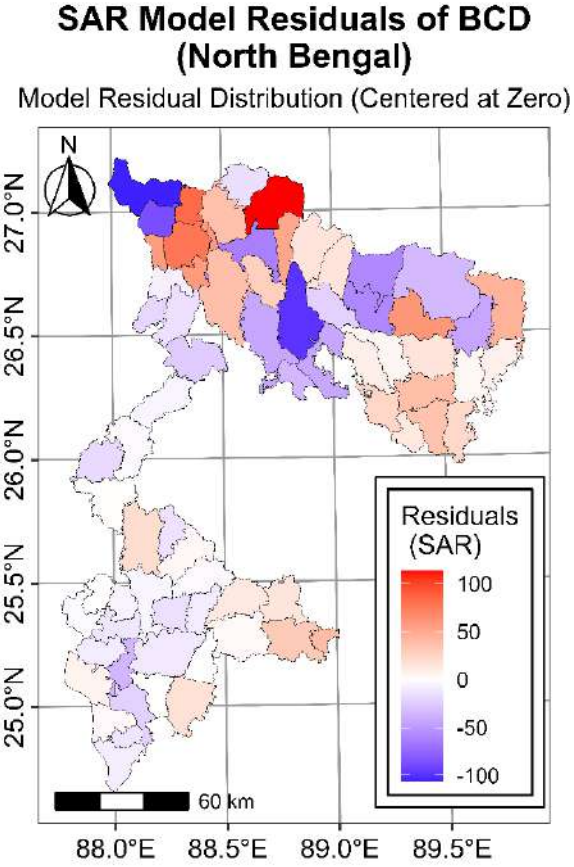

Figure 7: Spatial Autoregressive Model Predicted Carbon Density

Elevation and Rainfall- Both remain significant positive drivers ($p < 0.001$, $p = 0.024$, respectively). This confirms that the high-altitude, high-precipitation zones of the Himalayas are among the most ecologically productive carbon sinks.

NDVI- NDVI shows a highly significant positive correlation ($\beta = 313.532$, $p = 0.005$), which validates its use as a robust biophysical proxy for monitoring BCD changes via remote sensing.

Shift in Climatic Sensitivity- In the SAR model, temperature—which was highly significant in the OLS model—is no longer statistically significant ($p = 0.120$). This suggests that its OLS effect was likely a proxy for spatial location, ceasing to be a primary driver once spatial connectivity among blocks is accounted for.

The SAR model outperforms OLS, as evidenced by higher log-likelihood (improved fit), lower AIC (greater parsimony), reduced Sigma2 (residual variance), and non-significant LM residual p-value (indicating the elimination of spatial autocorrelation).

This SAR model exhibits that the BCD in North Bengal depends not only on some local geospatial factors like tree cover and elevation, but also is significantly influenced by the biomass behaviour of neighbouring CD blocks. This reveals the need for a landscape-level conservation plan, because forest degradation in one block will adversely affect the carbon sequestration potential of neighbouring blocks.

In spatial econometric modelling, however, the coefficients of the SAR model is not interpreted directly as the marginal effects because of spatial feedback loops. The total effect of a covariate is decomposed into direct, indirect and total effects instead.

The distribution of residuals from the Spatial Autoregressive model for North Bengal, as shown in the provided map [Figure 6], indicates a strong overall model fit whose mean is cantered at zero. By incorporating a spatial lag coefficient ($\rho = 0.295$), the model has successfully mitigated the systematic spatial clustering typical of standard global regression models in this region.

G. Spatial Patterns of BCD

Southern CD Blocks- CD blocks in the southern districts (e.g., North and South Dinajpur, Malda) primarily exhibit white or pale shading Figure 7. These areas correspond to the flat alluvial plains [1] where residuals are near-zero, signifying that the model's predictors (such as tree cover and NDVI) provide highly accurate estimates for these relatively homogeneous agricultural and urbanizing landscapes.

Northern Hilly Region- The highest residual variance is shown by the northernmost Community Development CD blocks, comprising a number of pockets depicting dark red and dark blue shading in the Himalayan highlands. This heterogeneity suggests that in the heterogeneous montane topography localized ecological drivers of biomass carbon density—such as microclimates or distinct montane ecotypes—cannot be fully captured by the parameters used in a global model.

It can also be seen that spatial autocorrelation in the residuals has been removed, highlighting the effectiveness of the SAR model, where systematic "High-High" & "Low-Low" clusters were present for BCD, much more random distribution is visible over this residual map. This

move enables BCD estimates to be statistically valid at the block level for territorial planning in North Bengal.

The spatial characterization of model errors shown by the residual map (Figure 7) shows that except for southern agricultural blocks which have near-perfect fit rest of the areas in Himalayan range show minor localized error resulting from heterogeneous terrain.

H. Impact Analysis and Spatial Spillovers of Carbon Drivers

The analysis reveals a highly consistent spillover pattern across all biophysical, anthropogenic, and physical variables. The indirect effects consistently constitute approximately 27.8% of the total impact for the primary drivers of carbon density. For instance, the indirect spillover for Tree Cover is 16,318.505 (out of a total impact of 58,666.557, or ~27.8%). Similarly, for NDVI (Indirect: 123.71; Total: 444.747) and Built-up Area (Indirect: -14,454.814; Total: -51,966.411), the spatial spillover remains fixed at roughly 27.8%. This mathematical consistency substantiates that carbon sequestration in North Bengal is a regional phenomenon rather than a strictly localized process, with nearly 28% of the carbon change in any given CD block mediated by the characteristics of its neighbours (see table 6).

Table 6: Quantifying the Impact of Biophysical and Anthropogenic Drivers on Regional Carbon Stocks

Variable	Direct Effect	Indirect Effect	Total Effect
NDVI	321.038**	123.71.	444.747**
BUTC	-37511.598*	-14454.814.	-51966.411*
TREE	42348.052***	16318.505*	58666.557***
RAIN	0.059*	0.023.	0.082*
TEMP	-13.735	-5.293	-19.028
ELVN	0.121***	0.046*	0.167***
Significance: *** p<0.001, ** p<0.01, * p<0.05, . p<0.1			

TREE:- The tree-covered area (TREE) has direct effect (β= 〖42,348.052〗 ^(***)), which signifies that the increase of 1 unit of tree coverage is the main local strategy for carbon sequestration. The indirect impact (β= 〖16,318.505〗 ^*) indicates that preserving forests within one block improves the ecological connectivity of neighboring units via positive spatial spillover effect.

BUTC- BUTC constitutes the primary driver of carbon diminution, with a total effect of β=- 〖51,966.411〗 ^* and direct effect of β=- 〖37,511.598〗 ^*}, elucidating the profound carbon cost associated with land urbanization. The indirect effect (β=-14,454.814) indicates that urban expansion within one block imposes negative externalities on neighboring Blocks, attributable to habitat fragmentation and edge effects linked to built-up corridors.

NDVI- The Normalized Vegetation Index (NDVI) further validates the effectiveness of remote sensing indices in monitoring biomass carbon density. We find an overall effect of β= 〖444.747〗 ^(**) (direct: β= 〖321.038〗 ^(**); indirect: β= 123.71) meaning that increased vegetation vigour and greenness is associated with greater biomass accumulation across the board. The positive indirect effect is attributed to the spatial continuity of vigorous vegetation between administrative regions.

ELVN- Elevation (ELVN) serves as a critical abiotic driver in the Himalayan terrain. The positive total effect (β= 〖0.167〗 ^(***);direct: β= 〖0.121〗 ^(***)}; indirect: β= 〖0.046〗 ^*) corroborates an association between higher elevations and increased biomass density, as elevation regulates moisture availability and restricts anthropogenic interference.

RAIN- Rain exhibits a positive total effect (β= 〖0.082〗 ^*; direct:β= 〖0.059〗 ^*}; indirect: $\beta = 0.023$), whereby adequate precipitation enhances primary productivity. The positive, albeit modest, indirect effect demonstrates the shared characteristics of climatic zones.

TEMP- Temperature (TEMP) has a negative total effect(β= -19.028; direct: β= -13.735; indirect: β= -5.293) as high BCD is less likely at hot temperatures in the southern plains than cold temperatures in the northern montane zones. The change in importance of temperature from the OLS to the SAR model indicates that its impact is mediated by spatial location.

The results of this impact analysis provide a strong statistical basis for a landscape-level conservation framework. As approximately 28% of the total impact of these variables occurs through spatial spillovers, traditional block-by-block management is insufficient. The "spillover economy" of carbon sequestration in North Bengal necessitates trans-boundary cooperation between administrative Blocks to maintain the integrity of the northern carbon core while mitigating the radiating negative impacts of urbanization in the southern plains.

VI. DISCUSSION

The following discussion evaluates the findings from the spatial analysis of Biomass Carbon Density across the 72 administrative Blocks of North Bengal and interprets the results within the context of regional geography and spatial econometric theory.

A. Spatial Autocorrelation and Model Validity

The Global Moran's I value of 0.7984 ($p < 0.001$) provides robust statistical evidence that BCD in North Bengal is not randomly distributed but exhibits strong positive spatial clustering. The concentration of High-High clusters in the northern mountainous Blocks signifies a "carbon core" where dense vegetation in one administrative unit enhances the biomass potential of its neighbours.

The transition from Ordinary Least Squares to the Spatial Autoregressive model was essential because OLS assumes independent observations("Uncertainty Modelling: Fundamental Concepts and Models," 2022), a condition violated by the significant spatial autocorrelation found in this region. By inclusion the spatial lag coefficient (ρ= 0.295), the model effectively accounts for the spatial dependency, as neighbouring features influence BCD values. This methodological shift secures more reliable estimates for block-level planning, particularly in the complex terrain, like Himalayan where global models often fail to capture localized variation.

B. Regional Hotspots and Climatic Gradient

These areas are characterized by multi-tier vegetation and favourable moisture conditions, as evidenced by the

positive total effect of rainfall (β= 〖0.082〗 ^*). The altitudinal gradient is a primary driver here; higher elevations regulate moisture and limit anthropogenic interference, thereby supporting greater carbon stocks.

Conversely, the "coldspots" in the southern plains, such as Tapan and Gangarampur, highlight the regional impact of intensive agriculture and urbanization on the Indo-Gangetic alluvium. In these southern CD blocks, the conversion of natural vegetation to cropland and built-up surfaces has significantly depleted the per-unit carbon storage.

C. Drivers of Carbon Dynamics and Spatial Spillovers

The decomposition of effects into direct and indirect impacts reveals that approximately 28% of the total impact of carbon drivers is realized through spatial spillovers.

D. Tree Cover and Vegetation Vigor

TREE (β= 〖58,666.557〗 ^(***)) and also NDVI (β= 〖 444.747〗 ^(**)}) are the most important positive predictors. The positive indirect effects signify that forest conservation in one block provides ecological externalities (e.g., micro-climatic stability and habitat connectivity) to adjacent CD blocks.

E. Urbanization Pressure

The significant negative impact of built-up area underscores the carbon cost of land-use conversion. The negative indirect effect suggests that urban expansion in one block—such as Matigara or Rajganj—imposes "fragmentation shocks" on the carbon potential of neighbouring rural CD blocks.

F. Climatic Sensitivity

The insignificance of temperature in the SAR model compared to the OLS model indicates that temperature's influence is largely mediated by spatial and altitudinal positioning.

VII. CONCLUSION

This research demonstrates that biomass carbon density in North Bengal is governed by a robust spatial clustering regime, which fundamentally challenges traditional non-spatial assessments of regional carbon stocks. The analysis confirms substantial positive spatial autocorrelation (Moran's I = 0.7984, $p < 0.001$), indicating that BCD is not a localized independent variable but an integral component of a contiguous ecological system. The delineation of a primary "carbon core" in the northern Himalayan Blocks, in contrast to "carbon depletion zones" in the southern plains, underscores geographic proximity as a dominant determinant of carbon storage capacity.

Furthermore, this study demonstrates the inadequacy of ordinary least squares regression for regional biomass modelling. Significant spatial dependence in the residuals confirms that OLS produces biased estimates by disregarding inter-block interactions that characterize North Bengal's landscape. Through the implementation of the spatial autoregressive model, this research quantifies a 28% spatial spillover effect (ρ≈0.295). This finding is critical, as it indicates that approximately 28% of a block's carbon density is influenced by the environmental health and conservation status of neighboring Blocks. Consequently, carbon sequestration emerges as a regional spillover benefit rather than a purely localized outcome.

As the first block-level spatial econometric analysis of BCD in North Bengal, this study establishes a novel empirical baseline for sub-regional climate policy. The results demonstrate that isolated conservation efforts within individual administrative units are insufficient; rather, the 28% spillover effect necessitates a trans-boundary landscape management approach. To preserve the integrity of North Bengal's carbon reservoirs, policy interventions must shift from block-level targets to integrated corridor-based strategies that account for the identified spatial dependencies[27].

VIII. POLICY RECOMMENDATIONS

A. Implement Trans-Boundary Forest Management Based on Spatial Spillovers

As this research identifies a significant spatial lag coefficient (ρ= 0.295), carbon density is not an isolated local attribute but a regional phenomenon. Given that approximately 28% of the total impact of carbon drivers manifests through spatial spillovers, administrative blocks cannot manage forests in isolation. The West Bengal Forest Department is recommended to adopt a landscape-level management model, coordinating conservation efforts in high-density CD Blocks, such as Gorubathan, with adjacent Blocks to sustain the regional spillover benefits of carbon sequestration.

B. Prioritize High-Altitude Carbon Sinks Based on the Dominant Effect of Tree Cover

The TREE variable exhibited the highest total effect (β= 58,666.557) in the model, confirming that forest density is the predominant driver of regional BCD. Given the High-High clusters identified in the northern Himalayan front, policies must establish strictly prohibited development zones for infrastructure development in these areas [10]. Forest loss in these core sinks would exert a disproportionately large negative impact on the North Bengal carbon pool due to the associated indirect effects.

C. Mitigate Fragmentation Effects from Urban Expansion

The model demonstrates that built-up area exerts a substantial negative total effect (β= -51,966.411). This implies that the carbon cost per unit of urban expansion is nearly equivalent to the benefit per unit of tree cover[28]. Urban planning in rapidly developing Blocks, such as Matigara and Rajganj, must therefore mandate green buffers to mitigate the negative indirect effects of urbanization, which impose fragmentation pressures on neighboring rural carbon stocks[28].

D. Targeted Restoration of Low-Low Coldspots

The identification of significant Low-Low coldspots in southern Blocks, such as Tapan and Gangarampur, provides a spatial framework for the Green India Mission. These areas should constitute the primary targets for agroforestry programmes.

CONFLICTS OF INTEREST

The authors declare that they have no conflicts of interest.

REFERENCES

1. Acharya, A., Mondal, B. K., Bhadra, T., Abdelrahman, K., Mishra, P. K., Tiwari, A., and Das, R., "Geospatial analysis of geo-ecotourism site suitability using AHP and GIS for sustainable and resilient tourism planning in West Bengal, India," *Sustainability*, vol. 14, no. 4, p. 2422, 2022. Available from: https://doi.org/10.3390/su14042422
2. Ahirwal, J., Nath, A., Brahma, B., Deb, S., Sahoo, U. K., Nath, A. J., and Nath, A. J., "Patterns and driving factors of biomass carbon and soil organic carbon stock in the Indian Himalayan region," *Science of the Total Environment*, vol. 770, p. 145292, 2021. Available from: https://doi.org/10.1016/j.scitotenv.2021.145292
3. Avtar, R., Aggarwal, R., Kharrazi, A., Kumar, P., and Kurniawan, T. A., "Utilizing geospatial information to implement SDGs and monitor their progress," *Environmental Monitoring and Assessment*, vol. 192, no. 1, 2019. Available from: https://doi.org/10.1007/s10661-019-7996-9
4. Behera, S. K., Sahu, N., Mishra, A. K., Bargali, S. S., Behera, M. D., and Tuli, R., "Aboveground biomass and carbon stock assessment in Indian tropical deciduous forest and relationship with stand structural attributes," *Ecological Engineering*, vol. 99, p. 513, 2016. Available from: https://doi.org/10.1016/j.ecoleng.2016.11.046
5. Bhattacharyya, C., Banerjee, S., Acharya, U., Mitra, A., Mallick, I., Haldar, A., Haldar, S., Ghosh, A., and Ghosh, A., "Evaluation of plant growth promotion properties and induction of antioxidative defense mechanism by tea rhizobacteria of Darjeeling, India," *Scientific Reports*, vol. 10, no. 1, 2020. Available from: https://doi.org/10.1038/s41598-020-72439-z
6. Cliff, A. D., and Ord, J. K., "Spatial autocorrelation," *Biometrics*, vol. 30, no. 4, p. 729, 1974. Available from: https://doi.org/10.2307/2529248
7. Deb, S., Debnath, M. K., Chakraborty, S., Weindorf, D. C., Kumar, D., Deb, D., and Choudhury, A., "Anthropogenic impacts on forest land use and land cover change: Modelling future possibilities in the Himalayan Terai," *Anthropocene*, vol. 21, p. 32, 2018. Available from: https://doi.org/10.1016/j.ancene.2018.01.001
8. Dormann, C. F., McPherson, J., Araújo, M. B., Bivand, R., Bolliger, J., Carl, G., Davies, R. G., Hirzel, A. H., Jetz, W., Kissling, W. D., Kühn, I., Ohlemüller, R., Peres-Neto, P. R., Reineking, B., Schröder, B., Schurr, F. M., and Wilson, R. J., "Methods to account for spatial autocorrelation in the analysis of species distributional data: A review," *Ecography*, vol. 30, no. 5, p. 609, 2007. Available from: https://doi.org/10.1111/j.2007.0906-7590.05171.x
9. Goswami, C. C., Mukhopadhyay, D., and Poddar, B. C., "Geomorphology in relation to tectonics: A case study from the eastern Himalayan foothills of West Bengal, India," *Quaternary International*, vol. 298, p. 80, 2012. Available from: https://doi.org/10.1016/j.quaint.2012.12.020
10. Hall, F. G., Bergen, K. M., Blair, J. B., Dubayah, R., Houghton, R. A., Hurtt, G. C., Kellndorfer, J., Lefsky, M. A., Ranson, J., Saatchi, S. S., Shugart, H. H., and Wickland, D. E., "Characterizing 3D vegetation structure from space: Mission requirements," *Remote Sensing of Environment*, vol. 115, no. 11, p. 2753, 2011. Available from: https://doi.org/10.1016/j.rse.2011.01.024
11. Hansen, M. C., Potapov, P., Moore, R., Hancher, M., Turubanova, S., Tyukavina, A., Thau, D., Stehman, S. V., Goetz, S. J., Loveland, T. R., Kommareddy, A., Egorov, A., Chini, L., Justice, C. O., and Townshend, J. R., "High-resolution global maps of 21st-century forest cover change," *Science*, vol. 342, no. 6160, p. 850, 2013. Available from: https://doi.org/10.1126/science.1244693
12. Huang, L., Yang, L., Tuyến, N. T., Colmekcioglu, N., and Jun, L., "Factors influencing the livelihood strategy choices of rural households in tourist destinations," *Journal of Sustainable Tourism*, vol. 30, no. 4, p. 875, 2021. Available from: https://doi.org/10.1080/09669582.2021.1903015
13. Kafy, A.-A., Saha, M., Fattah, Md. A., Rahman, M. T., Duti, B. M., Rahaman, Z. A., Bakshi, A., Kalaivani, S., Rahaman, S. N., and Sattar, G. S., "Integrating forest cover change and carbon storage dynamics: Leveraging Google Earth Engine and InVEST model to inform conservation in hilly regions," *Ecological Indicators*, vol. 152, p. 110374, 2023. Available from: https://doi.org/10.1016/j.ecolind.2023.110374
14. Kaushal, S., and Baishya, R., "Stand structure and species diversity regulate biomass carbon stock under major Central Himalayan forest types of India," *Ecological Processes*, vol. 10, no. 1, 2021. Available from: https://doi.org/10.1186/s13717-021-00283-8
15. Kelejian, H. H., and Prucha, I. R., "Specification and estimation of spatial autoregressive models with autoregressive and heteroskedastic disturbances," *Journal of Econometrics*, vol. 157, no. 1, p. 53, 2009. Available from: https://doi.org/10.1016/j.jeconom.2009.10.025
16. Kijowska-Strugała, M., Baran, A., Szara-Bąk, M., Wiejaczka, Ł., and Prokop, P., "Soil quality under different agricultural land uses as evaluated by chemical, geochemical and ecological indicators in mountains with high rainfall (Darjeeling Himalayas, India)," *Journal of Soils and Sediments*, vol. 22, no. 12, p. 3041, 2022. Available from: https://doi.org/10.1007/s11368-022-03274-0
17. Legendre, P., "Spatial autocorrelation: Trouble or new paradigm?" *Ecology*, vol. 74, no. 6, p. 1659, 1993. Available from: https://doi.org/10.2307/1939924
18. Mitra, S., and Mukherjee, S. K., "Observation on traditional treatment methods of furuncle and carbuncle by tribal people of North Bengal plains of West Bengal, India," *Plant Archives*, vol. 22, no. 2, p. 512, 2022. Available from: https://doi.org/10.51470/plantarchives.2022.v22.no2.092
19. Murray, B. C., McCarl, B. A., and Lee, H., "Estimating leakage from forest carbon sequestration programs," *Land Economics*, vol. 80, no. 1, p. 109, 2004. Available from: https://doi.org/10.2307/3147147
20. Pan, Y., Birdsey, R. A., Phillips, O. L., Houghton, R. A., Fang, J., Kauppi, P. E., Keith, H., Kurz, W. A., Ito, A., Lewis, S. L., Nabuurs, G. J., Shvidenko, A., Hashimoto, S., Lerink, B., Schepaschenko, D., Castanho, A., and Murdiyarso, D., "The enduring world forest carbon sink," *Nature*, vol. 631, no. 8021, p. 563, 2024. Available from: https://doi.org/10.1038/s41586-024-07602-x
21. Prokop, P., and Walanus, A., "Impact of the Darjeeling–Bhutan Himalayan front on rainfall hazard pattern," *Natural Hazards*, vol. 89, no. 1, p. 387, 2017. Available from: https://doi.org/10.1007/s11069-017-2970-8
22. Qi, Y., Zhang, Y., Wang, K., He, S., and Tan, W., "Application of spatial regression models for forest biomass estimation in Guizhou Province, Southwest China," *Applied Ecology and Environmental Research*, vol. 18, no. 5, p. 7215, 2020. Available from: https://doi.org/10.15666/aeer/1805_72157232
23. Rajashekar, G., Fararoda, R., Reddy, R. S., Jha, C. S., Ganeshaiah, K. N., Singh, J. S., and Dadhwal, V. K., "Spatial distribution of forest biomass carbon (above and below ground) in Indian forests," *Ecological Indicators*, vol. 85, p. 742, 2017. Available from: https://doi.org/10.1016/j.ecolind.2017.11.024
24. Rishi, H., and Purkayastha, S., "Indicator-based assessment of coping and adaptive strategies against flood hazards in Tal and Diara regions of Malda District, West Bengal (India)," *Research Square*, 2020. Available from: https://doi.org/10.21203/rs.3.rs-52304/v1
25. Sarkar, A., Roy, D., and Mandal, D. K., "Assessment of spatial variability mapping of soil properties and its impacts on agricultural productivity using GIS approach in Siliguri sub-division, West Bengal, India," *Current World*

Environment, vol. 18, no. 2, p. 795, 2023. Available from: https://doi.org/10.12944/cwe.18.2.28

26. Schwarz, K., Fragkias, M., Boone, C. G., Zhou, W., McHale, M. R., Grove, J. M., O'Neil-Dunne, J., McFadden, J. P., Buckley, G. L., Childers, D. L., Ogden, L. A., Pincetl, S., Pataki, D. E., Whitmer, A., and Cadenasso, M. L., "Trees grow on money: Urban tree canopy cover and environmental justice," *PLoS ONE*, vol. 10, no. 4, 2015. Available from: https://doi.org/10.1371/journal.pone.0122051
27. Spawn, S., Sullivan, C., Lark, T. J., and Gibbs, H., "Harmonized global maps of above and belowground biomass carbon density in the year 2010," *Scientific Data*, vol. 7, no. 1, 2020. Available from: https://doi.org/10.1038/s41597-020-0444-4
28. Wang, Q., Ni, J., and Tenhunen, J., "Application of a geographically weighted regression analysis to estimate net primary production of Chinese forest ecosystems," *Global Ecology and Biogeography*, vol. 14, no. 4, p. 379, 2005. Available from: https://doi.org/10.1111/j.1466-822x.2005.00153.x